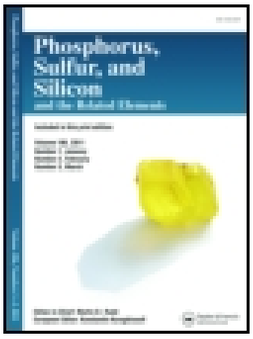

Phosphorus, Sulfur, and Silicon and the Related Elements

ISSN: 1042-6507 (Print) 1563-5325 (Online) Journal homepage: https://www.tandfonline.com/loi/gpss20

A novel and facile synthetic route to MMo (M = Ni or Co) bimetallic phosphides

Zhiwei Yao, Meijun Dong, Yan Shi, Yue Sun & Qingyou Liu

To cite this article: Zhiwei Yao, Meijun Dong, Yan Shi, Yue Sun & Qingyou Liu (2019): A novel and facile synthetic route to MMo (M=Ni or Co) bimetallic phosphides, Phosphorus, Sulfur, and Silicon and the Related Elements, DOI: 10.1080/10426507.2019.1660657

To link to this article: https://doi.org/10.1080/10426507.2019.1660657

PHOSPHORUS, SULFUR, AND SILICON AND THE RELATED ELEMENTS
https://doi.org/10.1080/10426507.2019.1660657

A novel and facile synthetic route to MMo (M = Ni or Co) bimetallic phosphides

Zhiwei Yao[a], Meijun Dong[a], Yan Shi[a], Yue Sun[a], and Qingyou Liu[b]

[a]College of Chemistry, Chemical Engineering and Environmental Engineering, Liaoning Shihua University, Fushun, People's Republic of China; [b]Key Laboratory of High-temperature and High-pressure Study of the Earth's Interior, Institute of Geochemistry, Chinese Academy of Sciences, Guiyang, People's Republic of China

ABSTRACT

A novel and facile route to bimetallic molybdenum phosphides was described. Both NiMoP and CoMoP phosphides were successfully prepared by a hexamethylenetetramine (HMT) route. Mixed-salt precursors containing HMT, M-HMT (M = Ni, Co or Mo) complexes, MMo-HMT (M = Ni or Co) complexes and P-containing species can be directly converted to bimetallic molybdenum phosphides under a flow of Ar at 800 °C. It was proposed that the bimetallic phosphides were formed via two possible reaction pathways: (i) MMo-HMT complexes/P→MMoP (M = Ni or Co) and (ii) M-HMT (M = Ni, Co or Mo) complexes/P→M_2P/MoP→MMoP (M = Ni or Co). Additionally, it was found that the dispersions and surface areas of NiMoP and CoMoP prepared by HMT route were higher than those of corresponding bimetallic phosphides prepared by traditional H_2 reduction method.

ARTICLE HISTORY
Received 30 May 2019
Accepted 23 August 2019

KEYWORDS
Bimetallic molybdenum phosphide; NiMoP; CoMoP; hexamethylenetetramine; formation mechanism

GRAPHICAL ABSTRACT

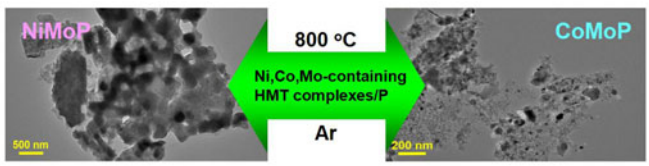

Introduction

After transition metal carbides and nitrides, transition metal phosphides are another class of interstitial compounds receiving much attention in recent years due to their widespread applications in various fields, such as electronics, photonics, magnetism, catalysis and so on.[1–4] In particular, metal phosphides (e.g. MoP, Ni_2P and Co_2P) have been identified as potential catalysts for many reactions such as hydrogenation and hydrotreating,[5–10] dry reforming of methane,[11] N_2H_4 decomposition,[12,13] NO dissociation[14] and electrocatalytic reactions including hydrogen evolution, oxygen reduction and evolution reactions.[15–17]. To further improve the catalytic activities of phosphide catalysts, M-based (M = Mo, Ni or Co) bimetallic phosphides have been prepared and used as catalysts. Recently, Zhang et al. investigated NiCo bimetallic phosphide catalyst for hydrogen evolution reaction (HER), and found that the NiCo bimetallic phosphide exhibited higher HER activity than their monometallic counterparts.[18] In addition, the synergistic effect between Ni and Co in the NiCo bimetallic phosphide system was also found in hydrodesulfurization (HDS) and hydrazine decomposition reactions.[19,20] Unlike NiCo bimetallic phosphide, no synergistic effect was observed between two metals in MMo (M = Ni or Co) bimetallic phosphides.[21,22] The HDS activity was found to be in the order of Ni_2P > MoP > NiMoP, and the hydrodeoxygenation (HDO) activities decreased in the sequence of Ni_2P > NiMoP > MoP.[21,22] However, the MMo (M = Ni or Co) bimetallic phosphide systems[5,21–28] were still studied widely in recent years probably due to the interesting bimetallic effects (e.g. regulating product distribution) for the phosphide systems in various reactions.[27]

Unlike monometallic phosphides that can be prepared using many methods including H_2-temperature programed reduction (H_2-TPR) of phosphate, chemical vapor deposition, phosphorization using red or white phosphorus, decomposition of high-boiling point tri-*n*-octylphosphine (TOP) or $P(SiMe_3)_3$ reported in several recent reviews,[1,28,29] the synthetic method for MMo (M = Ni or Co) bimetallic phosphides was limited to only one approach, viz. H_2-TPR method.[5,21–27] Therefore, it was worthwhile to develop novel and simple methods for the preparation of bimetallic phosphide catalysts.

In recent years, the main research focuses of our group were on the preparation and catalytic activity of phosphides.[30–40] We developed an original technique for the

CONTACT Qingyou Liu liuqingyou@vip.gyig.ac.cn Key Laboratory of High-temperature and High-pressure Study of the Earth's Interior, Institute of Geochemistry, Chinese Academy of Sciences, Guiyang, 550081, People's Republic of China.
Color versions of one or more of the figures in the article can be found online at www.tandfonline.com/gpss.
Supplemental data for this article can be accessed on the publisher's website.

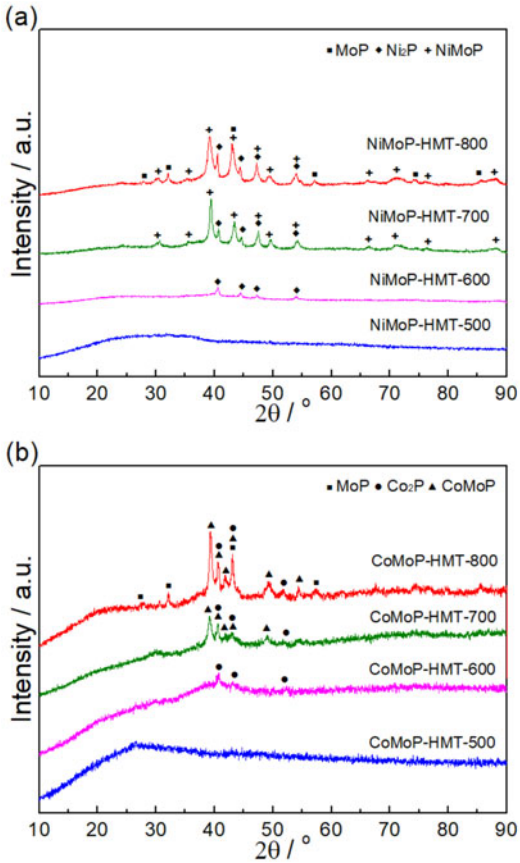

Figure 1. XRD patterns of the products of NiMoP-HMT (a) and CoMoP-HMT (b) thermal decomposition at different temperatures.

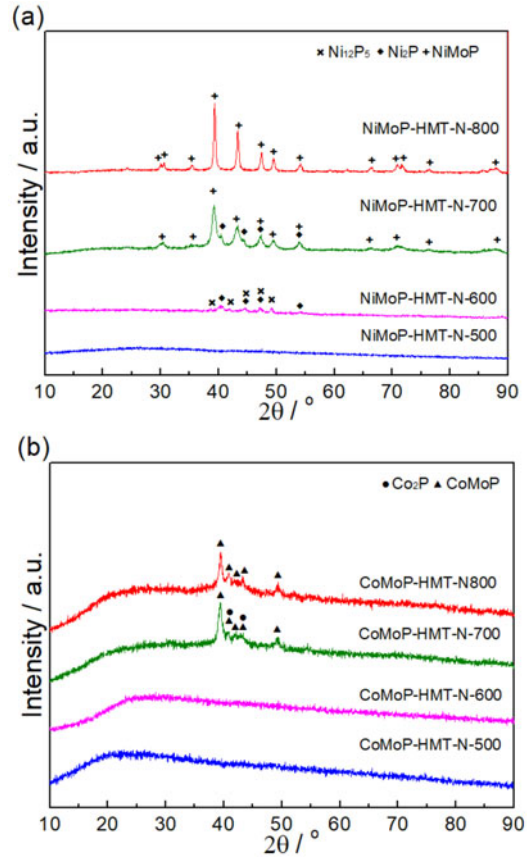

Figure 2. XRD patterns of the products of NiMoP-HMT-N (a) and CoMoP-HMT-N (b) thermal decomposition at different temperatures.

synthesis of highly dispersed monometallic phosphides (MoP, Ni_2P and Co_2P) by one-step decomposition of hexamethylenetetramine (HMT)-containing precursors under inert atmosphere.[39,40] This HMT-based method produced CO as major gas product rather than H_2O. The high dispersions and surface areas of as-prepared phosphides were achieved probably owing to the mitigation of hydrothermal sintering. Based on the success with the HMT route to synthesize monometallic phosphides, we decided to attempt whether this simple procedure can also be used to produce bimetallic phosphides. In this work, both NiMoP and CoMoP phosphides were successfully prepared by the HMT route. Techniques of XRD, XPS, TEM, SEM and EDX element mapping were adopted for the characterization of products and precursors, to give insights into the formation mechanism of bimetallic phosphides.

Results and discussion

Figure 1 shows the XRD patterns of the products of the NiMoP-HMT and CoMoP-HMT precursors decomposition at different temperatures. After decomposition at 500 °C, the resulting samples NiMoP-HMT-500 and CoMoP-HMT-500 were completely amorphous. When the temperature was increased to 600 °C, there were poorly crystalline Ni_2P (main diffraction peaks at $2\theta = 40.6°$, 44.5°, 47.3° and 54.1°, PDF 65-1989) and Co_2P (main diffraction peaks at $2\theta = 40.8°$, 43.3° and 52.1°, PDF 32-0306) generated on the NiMoP-HMT-600 and CoMoP-HMT-600 samples, respectively. With a further increase of temperature to 700 °C, an additional new set of peaks for NiMoP (main diffraction peaks at $2\theta = 39.2°$, 43.2°, 47.3°, 49.2° and 54.2°, PDF 71-0202) and CoMoP (main diffraction peaks at $2\theta = 39.2°$, 40.8°, 41.6°, 42.9° and 47.0°, PDF 71-0478) appeared on the NiMoP-HMT-700 and CoMoP-HMT-700 samples, respectively. At the final temperature of 800 °C, both NiMoP-HMT-800 and CoMoP-HMT-800 samples showed three mixed phases of MoP (main diffraction peaks at $2\theta = 27.9°$, 32.0°, 43.0° and 57.1°, PDF 65-6487), Ni_2P, NiMoP and MoP, Co_2P and CoMoP, respectively.

Table 1. Phase structures of the solid products during decomposition processes.

NiMo sample	XRD phases	CoMo sample	XRD phases
NiMoP-HMT-500	Amorphous	CoMoP-HMT-500	Amorphous
NiMoP-HMT-600	Ni_2P	CoMoP-HMT-600	Co_2P
NiMoP-HMT-700	NiMoP, Ni_2P	CoMoP-HMT-700	CoMoP, Co_2P
NiMoP-HMT-800	NiMoP, Ni_2P, MoP	CoMoP-HMT-800	CoMoP, Co_2P, MoP
NiMoP-HMT-N-500	Amorphous	CoMoP-HMT-N-500	Amorphous
NiMoP-HMT-N-600	Ni_2P, $Ni_{12}P_5$	CoMoP-HMT-N-600	Amorphous
NiMoP-HMT-N-700	NiMoP, Ni_2P	CoMoP-HMT-N-700	CoMoP, Co_2P
NiMoP-HMT-N-800	NiMoP	CoMoP-HMT-N-800	CoMoP

Figure 2 shows the XRD patterns of the products of the precursors with added $NH_3{\cdot}2H_2O$ (NiMoP-HMT-N and CoMoP-HMT-N) decomposition at different temperatures. Like the products of MMoP-HMT decomposition at low temperatures (500–700 °C), the products of MMoP-HMT-N

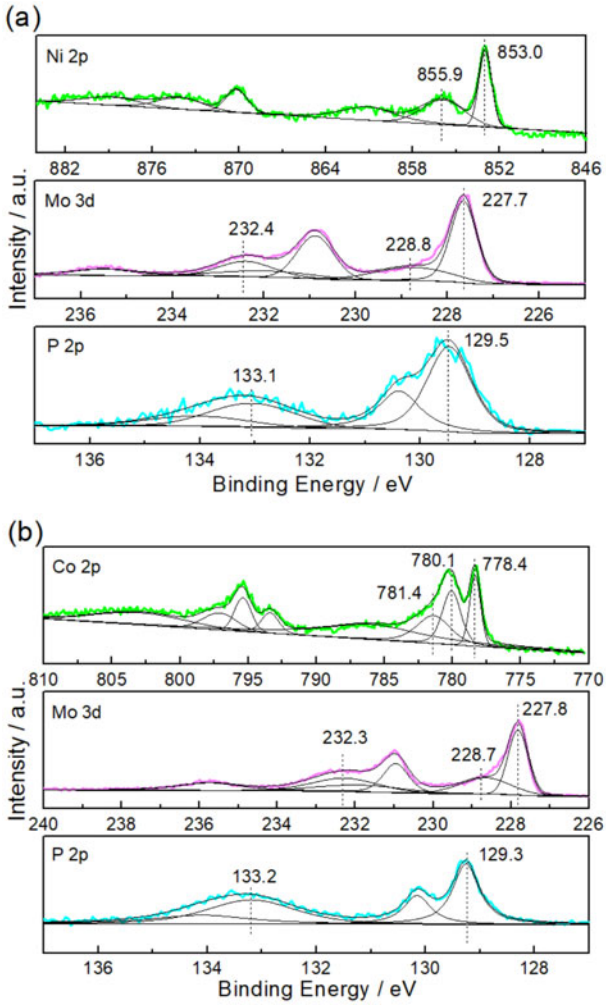

Figure 3. XPS spectra of Ni 2p, Co 2p, Mo 3d and P 2p: (a) NiMoP-HMT-N-800; (b) CoMoP-HMT-N-800.

decomposition also showed a phase transformation: amorphous state→M phosphide→M phosphide and MMo phosphide mixture (M = Ni or Co). Fortunately, however, unlike MMoP-HMT-800 samples were mixed phases of MMo bimetallic phosphides and their monometallic counterparts, the MMoP-HMT-N-800 samples demonstrated the single phases of MMoP (M = Ni or Co). For the sake of comparison, Table 1 summarizes the phase structures of the solid products obtained during decomposition processes. It was obvious from Table 1 that the addition of $NH_3{\cdot}2H_2O$ in the precursor preparation was helpful for the formation of single phases of MMoP (M = Ni or Co).

To further confirm the formation of MMoP, the MMoP-HMT-N-800 (M = Ni or Co) samples were characterized by XPS, SEM, TEM and so on. Figure 3 shows the XPS spectra of Ni 2p, Co 2p, Mo 3d and P 2p levels for the MMoP-HMT-N-800 (M = Ni or Co) samples. Based on the curve fitting, the binding energies of Ni $2p_{3/2}$, Co $2p_{3/2}$, Mo $3d_{5/2}$ and P $2p_{3/2}$ and the distribution of these corresponding species are listed in Table 2. It can be seen from Figure 3 and Table 2 that the surface regions of the two samples were composed of oxidized species and phosphorized species. The binding energies of oxidized Ni (855.9 eV), Co (780.1 and 781.4 eV) Mo (228.7–228.8 and 232.3–232.4 eV) and P (133.1–133.2 eV) were agreed with assignments by others to Ni^{2+}, $Co^{2+/3+}/Co^{2+}$, Mo^{4+}/Mo^{6+} and P^{5+} species,[41–43] respectively. The binding energies of the peaks at 853.0, 778.4, 227.7–227.8 and 129.3–129.5 eV were attributed to $Ni^{\alpha+}$, $Co^{\beta+}$, $Mo^{\delta+}$ and $P^{\sigma-}$ in phosphide,[27,39] respectively. The detection of these oxidized species was attributed to surface oxidation of phosphides in the passivation process.[42] In addition, the XPS of O 1s for the bimetallic phosphide samples might be also of interests and the results were shown in Supplemental Material, Figure S1. The region of the O 1s spectra included three peaks. It was suggested that peaks at 530.9–531.0 and 532.3–532.4 eV were due to metal oxides and PO_x,[44,45] respectively, and those at about 533.1 eV to adsorbed oxygen species such as O^-, OH^- or H_2O.[45]

Subsequently, the morphologies of MMoP-HMT-N-800 (M = Ni or Co) samples were investigated by SEM and TEM. It can be observed from SEM images (Figure 4) that the morphologies of NMoP-HMT-N-800 and CoMoP-HMT-N-800 were similar and they were composed of nanoparticles with size range of around 50–200 and 10–100 nm, respectively. Additionally, it was obvious that these nanoparticles connected with each other through thin plates or sheets. These plates or sheets should be carbon deposits from HMT decomposition, as suggested before.[39] These results were in good accordance with the observation of TEM images (Figure 5). The insets in Figure 5 clearly showed the crystal lattices of NiMoP (111) and CoMoP (201), which further proved the existence of NiMoP and CoMoP in the NMoP-HMT-N-800 and CoMoP-HMT-N-800 samples, respectively. For the sake of comparison, the morphologies of NiMoP and CoMoP prepared by traditional H_2-TPR method were also characterized by means of SEM. It can be seen from Supplemental Material, Figure S2 that the NiMoP and CoMoP consisted of large aggregates of irregularly shaped particles, which was similar to the result reported by others.[46] It was clear that the dispersions of NiMoP and CoMoP prepared by HMT route were higher than those of corresponding bimetallic phosphides prepared by H_2-TPR method (see Figure 4 and Supplemental Material, Figure S2).

Finally, the textural properties and carbon contents of the NiMoP and CoMoP samples obtained in this study were listed in Table 3. It was found that the NiMoP and CoMoP phosphides obtained by HMT method showed lower BET surface areas than monometallic phosphides Ni_2P (S_{BET}=191.7 $m^2\ g^{-1}$ and carbon content = 32.5 wt%) and Co_2P (S_{BET}=43.6 $m^2\ g^{-1}$ and carbon content = 25.3 wt%),[39] probably attributing to their lower carbon contents. It was reported that the existence of a large amount of carbon in phosphide materials can play a role in bonding of nanoparticle aggregation, leading to the enhancement of surface area of phosphides.[47] Note that the surface areas of NiMoP and CoMoP prepared by HMT route were higher than those of corresponding bimetallic phosphides prepared by traditional H_2-TPR method (S_{BET}=8 $m^2\ g^{-1}$ for NiMoP and S_{BET}=5 $m^2\ g^{-1}$ for CoMoP).[5]

To understand the formation mechanism of NiMoP and CoMoP phosphides, the MMoP-HMT and MMoP-HMT-N

Table 2. XPS results of Ni 2p, Co 2p, Mo 3d and P 2p for the single phases of NiMoP and CoMoP obtained in this study.

	Binding energy (eV)									
	Mo $3d_{5/2}$			Ni $2P_{3/2}$		Co $2P_{3/2}$			P $2p_{3/2}$	
Sample	$Mo^{\delta+}$	Mo^{4+}	Mo^{6+}	$Ni^{\alpha+}$	Ni^{2+}	$Co^{\beta+}$	$Co^{2+/3+}$	Co^{2+}	$P^{\sigma-}$	P^{5+}
NiMoP-HMT-N-800	227.7	228.8	232.4	853.0	855.9				129.5	133.1
CoMoP-HMT-N-800	227.8	228.7	232.3			778.4	780.1	781.4	129.3	133.2

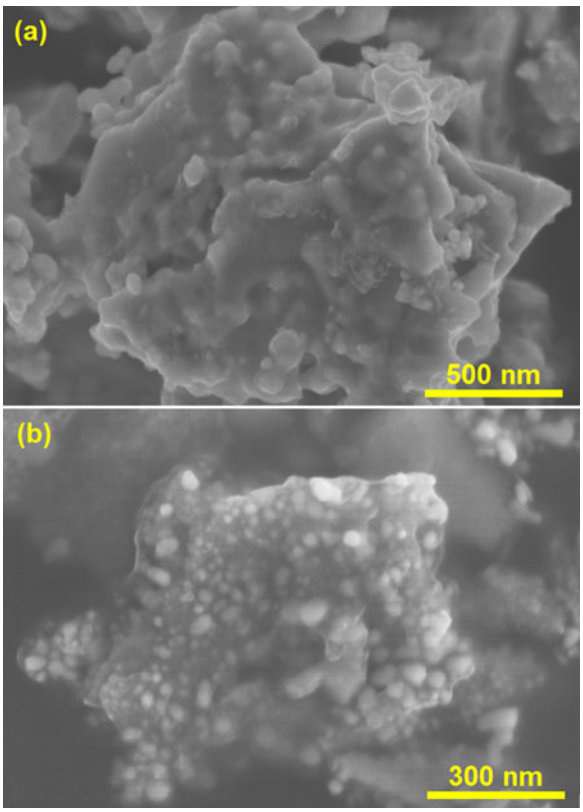

Figure 4. SEM images of (a) NiMoP-HMT-N-800 and (b) CoMoP-HMT-N-800.

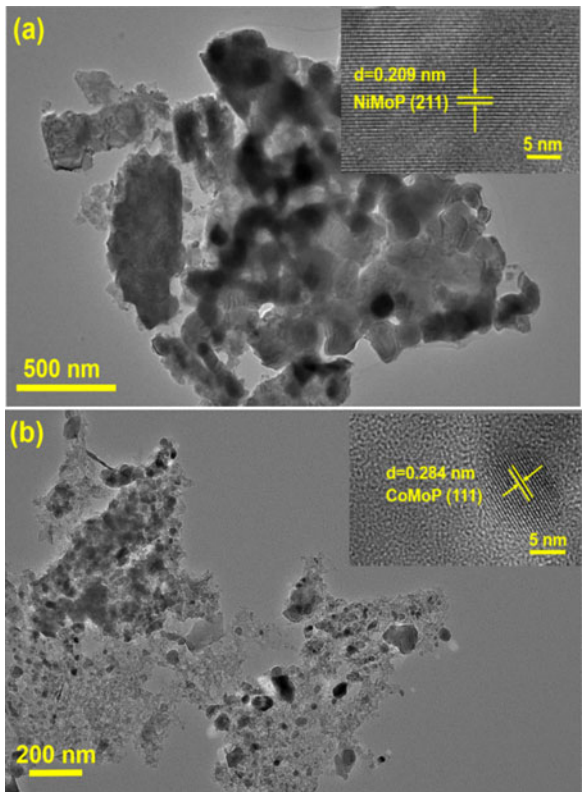

Figure 5. TEM images of (a) NiMoP-HMT-N-800 and (b) CoMoP-HMT-N-800. The insets show the corresponding NiMoP (211) and CoMoP (111) crystal lattices.

(M = Ni or Co) precursors were characterized by XRD and EDX element mapping. Figure 6 shows the XRD patterns of these MMoP-HMT and MMoP-HMT-N (M = Ni or Co) precursors as well as HMT for comparison. It can be seen from Figure 6 that the MMoP-HMT and MMoP-HMT-N (M = Ni or Co) precursors contained unknown compounds except M-HMT (M = Ni, Co or Mo) complexes (the phases shown in Supplemental Material, Figure S3 have been confirmed by our previous study)[30] and HMT itself. The unidentified phases were likely to be MMo (M = Ni or Co) complexes with HMT, as proved by others.[48] And the lack of P-containing phases on the XRD patterns of MMoP-HMT and MMoP-HMT-N (M = Ni or Co) precursors was due to these P-containing compounds being fully amorphous.[39] Therefore, it can be deduced that the MMoP-HMT and MMoP-HMT-N (M = Ni or Co) precursors should be composed of M-HMT (M = Ni, Co or Mo) complexes, MMo-HMT (M = Ni or Co) complexes, P-containing species and HMT.

In view of the fact that the formation mechanism of monometallic phosphides was proposed as the in situ decomposition/reduction of MP-HMT (M = Ni, Co or Mo) precursors (composed of M-HMT (M = Ni, Co or Mo) complexes, P-containing species and HMT) to produce Ni_2P, Co_2P and MoP,[39,40] it was reasonable to observe from Figure 1 that the in situ decomposition/reduction of MMoP-HMT precursors would yield mixtures of M_2P, MoP and MMoP (M = Ni or Co). The formation temperatures of Ni_2P and Co_2P (>600 °C) were lower than that of MoP (800 °C), which agreed with the results of previous studies.[39,40] It was reasonable to deduce that the MMoP should be originated from the decomposition/reduction of MMo-HMT (M = Ni or Co) complexes and P-containing species. Noticeably, in the case of the MMoP-HMT-N precursors (Figure 2), although there was the existence of M_2P intermediates at temperatures below 700 °C, the final products were phase-pure MMoP (M = Ni or Co). Moreover, there was no formation of MoP phase when the MMoP-HMT-N (M = Ni or Co) precursors were heated at 800 °C. Therefore, it was possible that the MoP can be reacted with M_2P to form MMoP (M = Ni or Co). To further confirm this fact, the mechanical mixtures of M_2P (M = Ni or Co) and MoP

Table 3. Textural properties and carbon contents of the NiMoP and CoMoP samples obtained in this study.

Sample	S_{BET} (m^2 g^{-1})	D_P (nm)	V_P (cm^3 g^{-1})	Carbon (wt%)
NiMoP-HMT-N-800	12.8	12.9	0.03	1.9
CoMoP-HMT-N-800	22.3	28.3	0.05	5.3

S_{BET}=BET surface area; D_P=average pore diameter; V_P=total pore volume.

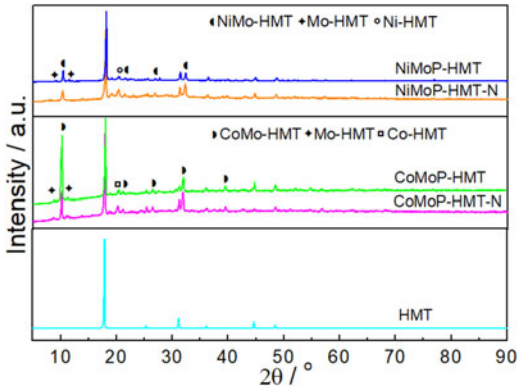

Figure 6. XRD patterns of MMoP-HMT and MMoP-HMT-N (M = Ni or Co) precursors as well as HMT for comparison.

were heated in H_2 at 800 °C and the resulting samples were characterized by XRD (Figures 7 and 8). It was found that the MoP can indeed react with Ni_2P/Co_2P to form Ni_xMo_yP[49] (main diffraction peaks at $2\theta = 40.3$, 44.3 and 47.3)/CoMoP. The solid–solid reactions were not complete, judging by the observed ratio of peaks intensities, which was probably due to weak interaction between solids formed in a simple mechanical mixing process. Thus, we proposed that the in situ decomposition/reduction of MMoP-HMT and MMoP-HMT-N precursors to produce MMoP (M = Ni or Co) via two possible reaction pathways: (i) MMo-HMT complexes/P→MMoP (M = Ni or Co) and (ii) M-HMT complexes (M = Ni, Co or Mo)/P→M_2P/MoP→MMoP (M = Ni or Co). In the case of monometallic phosphides, the $NH_3{\cdot}2H_2O$ was not necessary in the preparation of phase-pure Ni_2P and Co_2P via HMT route.[39] Although the $NH_3{\cdot}2H_2O$ was added in the preparation of MoP in our previous study,[40] this study result (not shown) indicated that the $NH_3{\cdot}2H_2O$ was not essential for the synthesis of phase-pure MoP via HMT method. It was worthy to note that the $NH_3{\cdot}2H_2O$ was crucially important to obtain phase-pure MMo (M = Ni or Co) bimetallic phosphides in this study. It was therefore interesting to investigate the effect of the addition of $NH_3{\cdot}2H_2O$ on the precursors in the preparation of MMo (M = Ni or Co) bimetallic phosphides.

Figure 9 shows the SEM images and EDX element mapping images of the MMoP-HMT and MMoP-HMT-N (M = Ni or Co) precursors, which confirmed the presence of M (M = Ni or Co), Mo and P elements, in agreement with the XPS results (Figure 3). Furthermore, it was clear that these elements were more uniformly distributed in the precursors with added $NH_3{\cdot}2H_2O$ than in the ones without added $NH_3{\cdot}2H_2O$. The results suggested that the dispersions of M-HMT (M = Ni, Co or Mo) complexes in the MMoP-HMT (M = Ni or Co) precursors was lower than those in the MMoP-HMT-N (M = Ni or Co) precursors. It was

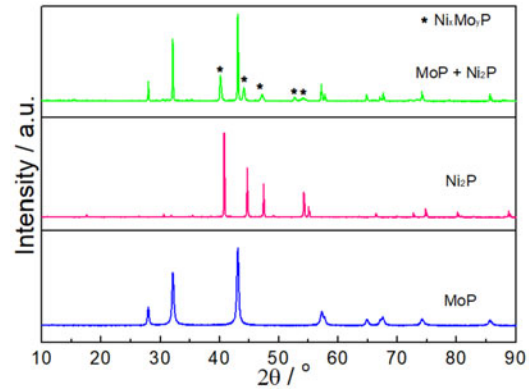

Figure 7. XRD pattern of mechanical mixture of Ni_2P and MoP (Ni:Mo = 1:1) treated in H_2 at 800 °C for 1 h. The patterns of Ni_2P and MoP are also shown for comparison.

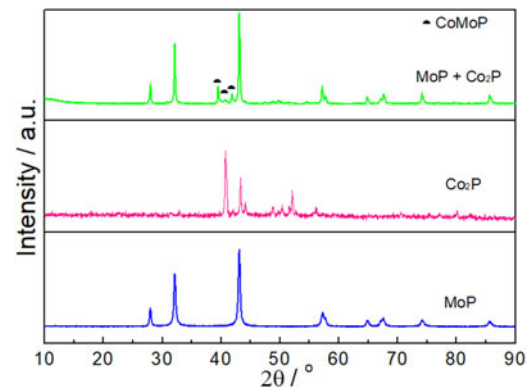

Figure 8. XRD pattern of mechanical mixture of Co_2P and MoP (Co:Mo = 1:1) treated in H_2 at 800 °C for 1 h. The patterns of Co_2P and MoP are also shown for comparison.

therefore reasonable that the transformation (M_2P/MoP→MMoP) was suppressed during decomposition/reduction of MMoP-HMT precursors, which led to the formation of mixtures of MMoP, M_2P and MoP (M = Ni or Co). In contrast, the MMoP-HMT-N (M = Ni or Co) precursors containing higher dispersed M-HMT (M = Ni, Co or Mo) complexes can be converted into phase-pure MMoP by the strong interaction between M_2P and MoP (M = Ni or Co).

Experimental

Sample preparation

The HMT precursors were prepared by dissolving $Ni(NO_3)_2{\cdot}6H_2O$ or $Co(NO_3)_2{\cdot}6H_2O$, $(NH_4)_6Mo_7O_{24}{\cdot}4H_2O$, $(NH_4)_2HPO_4$ and HMT ($N_4(CH_2)_6$) with a fixed mole ratio of M:Mo:P:HMT = 1:1:1:6 (M = Ni or Co). The solutions with some precipitate were kept under stirring at room temperature (RT) for 1 h and then dried at 110 °C. The resulting samples were designated as NiMoP-HMT and CoMoP-HMT, respectively. Additionally, to dissolve the precipitate, a few drops of ammonium hydroxide ($NH_3{\cdot}2H_2O$) were added in the solutions, and after stirred and dried the resulting samples were designated as NiMoP-HMT-N and CoMoP-HMT-N, respectively. The decomposition of precursors was carried out in a quartz reactor under a flow of Ar (50 mL min^{-1}). The temperature was raised linearly at a rate

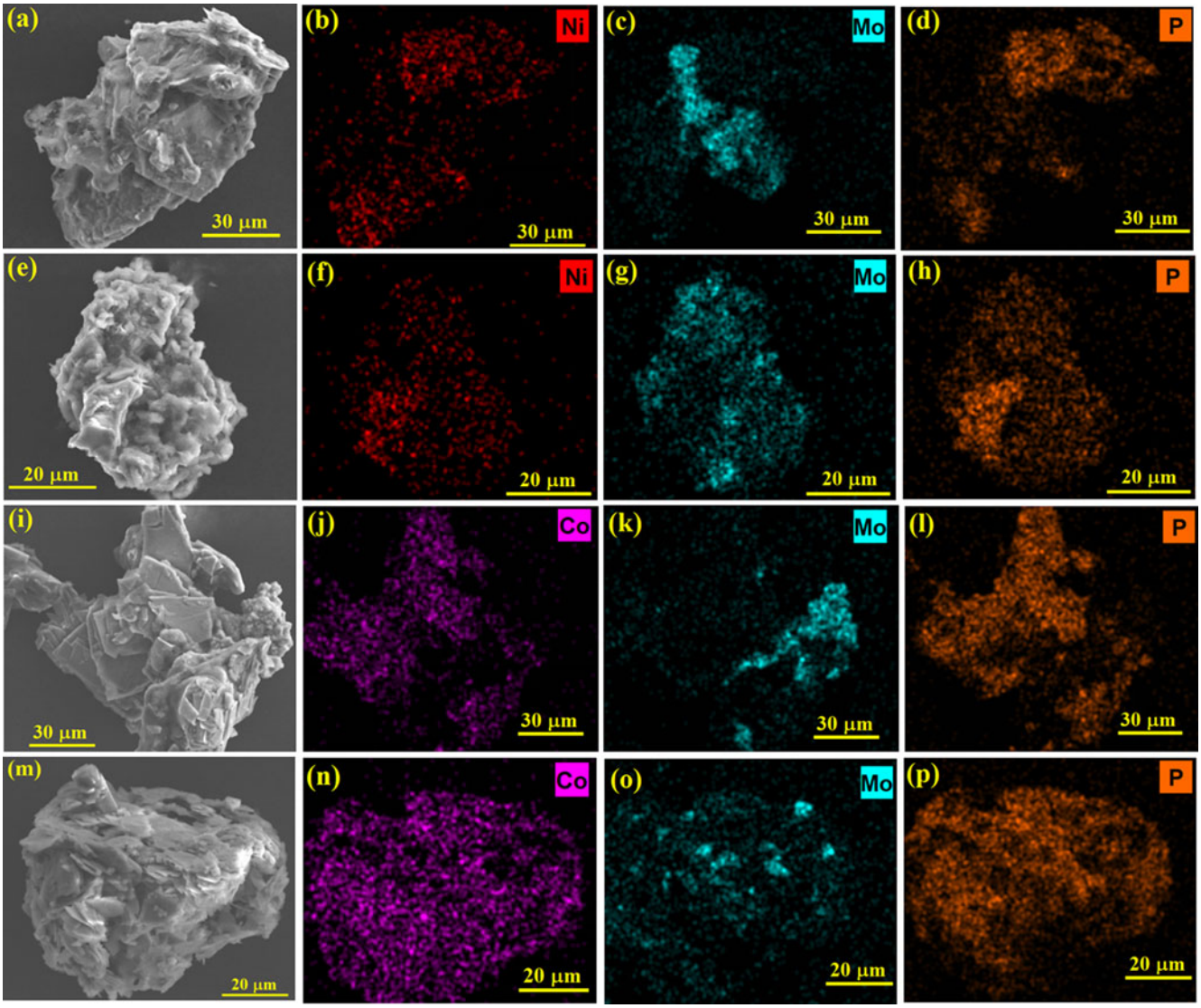

Figure 9. SEM images and the corresponding Ni, Co, Mo and P element mapping images of NiMoP-HMT (a–d), CoMoP-HMT (i–l), NiMoP-HMT-N (e–h) and CoMoP-HMT-N (m–p) precursors.

of 10 °C min^{-1} and kept at a given value for 1 h, followed by cooling to RT under Ar flow, and then passivated at RT in a flow of 1%O_2/Ar for 2 h. A series of samples were obtained from heating at 500, 600, 700 and 800 °C, designated as MMoP-HMT-T and MMoP-HMT-N-T (M = Ni or Co, T = 500, 600, 700 and 800).

Sample characterizations

X-ray diffraction (XRD) was carried out on an X-ray diffractometer (X'Pert Pro MPD) equipped with a Cu Kα source. X-ray photoelectron spectroscopy (XPS) investigation was conducted using a Kratos Axis ultra (DLD) equipped with Al Kα X-ray source. Charging effects were corrected by means of adventitious carbon (284.6 eV) referencing. The morphology of the samples was characterized by scanning electron microscopy (SEM, Hitachi S-4800) and transmission electron microscopy (TEM, Philips Tecnal 10). The energy dispersive X-ray spectroscopy (EDX) element mapping images were taken on the Hitachi S-4800 SEM unit. BET surface area of the samples was measured by a surface area analyzer (NOVA4200). Carbon content of the samples was determined by a Heraeus CHN-O-Rapid analyzer.

Conclusions

In summary, phase-pure NiMoP and CoMoP phosphides were successfully prepared by in situ decomposition/reduction of mixed-salt precursors containing HMT, M-HMT (M = Ni, Co or Mo) complexes, MMo-HMT (M = Ni or Co) complexes and P-containing species under a flow of Ar at 800 °C. The investigation of the formation process showed that the bimetallic phosphide phases were formed via two possible reaction pathways: (i) MMo-HMT complexes/P→MMoP (M = Ni or Co) and (ii) M-HMT (M = Ni, Co or Mo) complexes/P→M_2P/MoP→MMoP (M = Ni or Co). It was worthy to note that the addition of $NH_3{\cdot}2H_2O$ into the precursors favored dispersing M-HMT (M = Ni, Co or Mo) complexes and P-containing species, which can promote the formation of NiMoP and CoMoP via the second pathway. In addition, the dispersions and surface areas of as-prepared NiMoP and CoMoP were superior to those of corresponding

bimetallic phoshides prepared by traditional H_2-TPR method. The advantages of the resulting NiMoP and CoMoP bimetallic phosphide nanomaterials were worthwhile for further exploration.

Disclosure statement

No potential conflict of interest was reported by the authors.

Funding

The work was supported by the National Natural Science Foundation of China (No. 21978125), the Project of Liaoning Province Department of Education (No. L2017LZD003), the Program for Liaoning Innovative Talents in University (No. LR2018070), the Liaoning Province Natural Science Foundation (No. 20180551272) and the Public Welfare Project of Guizhou Province (No. 2016-09-1).

ORCID

Zhiwei Yao http://orcid.org/0000-0002-2535-9808
Qingyou Liu http://orcid.org/0000-0002-5630-7680

References

[1] Alexander, A.-M.; Hargreaves, J. S. J. Alternative Catalytic Materials: Carbides, Nitrides, Phosphides and Amorphous Boron Alloys. *Chem. Soc. Rev.* **2010**, *39*, 4388–4401. DOI: 10.1039/b916787k.

[2] Popczun, E. J.; McKone, J. R.; Read, C. G.; Biacchi, A. J.; Wiltrout, A. M.; Lewis, N. S.; Schaak, R. E. Nanostructured Nickel Phosphide as an Electrocatalyst for the Hydrogen Evolution Reaction. *J. Am. Chem. Soc.* **2013**, *135*, 9267–9270. DOI: 10.1021/ja403440e.

[3] Yoon, K. Y.; Jang, Y.; Park, J.; Hwang, Y.; Koo, B.; Park, J.-G.; Hyeon, T. Synthesis of Uniform-Sized Bimetallic Ironnickel Phosphide Nanorods. *J. Solid State Chem.* **2008**, *181*, 1609–1613. DOI: 10.1016/j.jssc.

[4] Jiang, X. C.; Xiong, Q. H.; Nam, S.; Qian, F.; Li, Y.; Lieber, C. M. InAs/InP Radial Nanowire Heterostructures as High Electron Mobility Devices. *Nano Lett.* **2007**, *7*, 3214–3218. DOI: 10.1021/nl072024a.

[5] Stinner, C.; Prins, R.; Weber, T. Binary and Ternary Transition-Metal Phosphides as HDN Catalysts. *J. Catal.* **2001**, *202*, 187–194. DOI: 10.1006/jcat.2001.3283.

[6] Wang, X.; Clark, P.; Oyama, S. T. Synthesis, Characterization, and Hydrotreating Activity of Several Iron Group Transition Metal Phosphides. *J. Catal.* **2002**, *208*, 321–331. DOI: 10.1006/jcat.2002.3604.

[7] Guan, Q.; Li, W. A Novel Synthetic Approach to Synthesizing Bulk and Supported Metal Phosphides. *J. Catal.* **2010**, *271*, 413–415. DOI: 10.1016/j.jcat.2010.02.031.

[8] Cecilia, J. A.; Infantes-Molina, A.; Rodríguez-Castellón, E.; Jiménez-López, A. Dibenzothiophene Hydrodesulfurization over Cobalt Phosphide Catalysts Prepared through a New Synthetic Approach: Effect of the Support. *Appl. Catal. B Environ.* **2009**, *92*, 100–113. DOI: 10.1016/j.apcatb.2009.07.017.

[9] Oyama, S. T. Novel Catalysts for Advanced Hydroprocessing: Transition Metal Phosphides. *J. Catal.* **2003**, *216*, 343–352. DOI: 10.1016/S0021-9517(02)00069-6.

[10] Oyama, S. T.; Gott, T.; Zhao, H.; Lee, Y. Transition Metal Phosphide Hydroprocessing Catalysts: A Review. *Catal. Today* **2009**, *143*, 94–107. DOI: 10.1016/j.cattod.2008.09.019.

[11] Yao, Z.; Luan, F.; Sun, Y.; Jiang, B.; Song, J.; Wang, H. Molybdenum Phosphide as a Novel and Stable Catalyst for Dry Reforming of Methane. *Catal. Sci. Technol.* **2016**, *6*, 7996–8004. DOI: 10.1039/C6CY00836D.

[12] Zheng, M.; Shu, Y.; Sun, J.; Zhang, T. Carbon-Covered Alumina: A Superior Support of Noble Metal-like Catalysts for Hydrazine Decomposition. *Catal. Lett.* **2008**, *121*, 90–96. DOI: 10.1007/s10562-007-9300-9.

[13] Cheng, R.; Shu, Y.; Zheng, M.; Li, L.; Sun, J.; Wang, X.; Zhang, T. Molybdenum Phosphide, a New Hydrazine Decomposition Catalyst: Microcalorimetry and FTIR Studies. *J. Catal.* **2007**, *249*, 397–400. DOI: 10.1016/j.jcat.2007.04.007.

[14] Yao, Z.; Dong, H.; Shang, Y. Catalytic Activities of Iron Phosphide for NO Dissociation and Reduction with Hydrogen. *J. Alloys Compd.* **2009**, *474*, L10–L13. DOI: 10.1002/chin.200925019.

[15] Lv, Y.; Wang, X. Nonprecious Metal Phosphides as Catalysts for Hydrogen Evolution, Oxygen Reduction and Evolution Reactions. *Catal. Sci. Technol.* **2017**, *7*, 3676–3691. DOI: 10.1039/C7CY00715A.

[16] Popczun, E. J.; Read, C. G.; Roske, C. W.; Lewis, N. S.; Schaak, R. E. Highly Active Electrocatalysis of the Hydrogen Evolution Reaction by Cobalt Phosphide Nanoparticles. *Angew. Chem.* **2014**, *126*, 5531–5534. DOI: 10.1002/anie.201402646.

[17] Feng, L.; Vrubel, H.; Bensimon, M.; Hu, X. Easily-Prepared Dinickel Phosphide (Ni_2P) Nanoparticles as an Efficient and Robust Electrocatalyst for Hydrogen Evolution. *Phys. Chem. Chem. Phys.* **2014**, *16*, 5917–5921. DOI: 10.1039/c4cp00482e.

[18] Zhang, R.; Wang, X.; Yu, S.; Wen, T.; Zhu, X.; Yang, F.; Sun, X.; Wang, X.; Hu, W. Ternary $NiCo_2P_x$ Nanowires as pH-Universal Electrocatalysts for Highly Efficient Hydrogen Evolution Reaction. *Adv. Mater.* **2017**, *29*, 1605502. DOI: 10.1002/adma.201605502.

[19] Abu, I. I.; Smith, K. J. The Effect of Cobalt Addition to Bulk MoP and Ni_2P Catalysts for the Hydrodesulfurization of 4,6-Dimethyldibenzothiophene. *J. Catal.* **2006**, *241*, 356–366. DOI: 10.1016/j.jcat.2006.05.010.

[20] Ding, L.; Shu, Y.; Wang, A.; Zheng, M.; Li, L.; Wang, X.; Zhang, T. Preparation and Catalytic Performances of Ternary Phosphides NiCoP for Hydrazine Decomposition. *Appl. Catal. A Gen.* **2010**, *385*, 232–237. DOI: 10.1016/j.apcata.2010.07.020.

[21] Wang, R.; Smith, K. J. Hydrodesulfurization of 4,6-Dimethyldibenzothiophene over High Surface Area Metal Phosphides. *Appl. Catal. A Gen.* **2009**, *361*, 18–25. DOI: 10.1016/j.apcata.2009.03.037.

[22] Li, K.; Wang, R.; Chen, J. Hydrodeoxygenation of Anisole over Silica-Supported Ni_2P, MoP, and NiMoP Catalysts. *Energy Fuels* **2011**, *25*, 854–863. DOI: 10.1021/ef101258j.

[23] Guichard, B.; Roy-Auberger, M.; Devers, E.; Legens, C.; Raybaud, P. Aging of Co(Ni)MoP/Al_2O_3 Catalysts in Working State. *Catal. Today* **2008**, *130*, 97–108. DOI: 10.1016/j.cattod.2007.09.007.

[24] Zuzaniuk, V.; Prins, R. Synthesis and Characterization of Silica-Supported Transition-Metal Phosphides as HDN Catalysts. *J. Catal.* **2003**, *219*, 85–96. DOI: 10.1016/S0021-9517(03)00149-0.

[25] Izhar, S.; Nagai, M. Transition Metal Phosphide Catalysts for Hydrogen Oxidation Reaction. *Catal. Today* **2009**, *126*, 172–176. DOI: 10.1016/j.cattod.2009.01.036.

[26] Nagai, M.; Fukiage, T.; Kurata, S. Hydrodesulfurization of Dibenzothiophene over Alumina-Supported Nickel Molybdenum Phosphide Catalysts. *Catal. Today* **2005**, *106*, 201–205. DOI: 10.1016/j.cattod.2005.07.130.

[27] Chen, J.; Yang, Y.; Shi, H.; Li, M.; Chu, Y.; Pan, Z.; Yu, X. Regulating Product Distribution in Deoxygenation of Methyl Laurate on Silica-Supported Ni-Mo Phosphides: Effect of Ni/Mo Ratio. *Fuel* **2014**, *129*, 1–10. DOI: 10.1016/j.fuel.2014.03.049.

[28] Callejas, J. F.; Read, C. G.; Roske, C. W.; Lewis, N. S.; Schaak, R. E. Synthesis, Characterization, and Properties of Metal Phosphide Catalysts for the Hydrogen-Evolution Reaction. *Chem. Mater.* **2016**, *28*, 6017–6044. DOI: 10.1021/acs.chemmater.6b02148.

[29] Carenco, S.; Portehault, D.; Boissiere, C.; Mezailles, N.; Sanchez, C. Nanoscaled Metal Borides and Phosphides: Recent Developments and Perspectives. *Chem. Rev.* **2013**, *113*, 7981–8065. DOI: 10.1021/cr400020d.

[30] Yao, Z.; Li, M.; Wang, X.; Qiao, X.; Zhu, J.; Zhao, Y.; Wang, G.; Yin, J.; Wang, H. A Novel Synthetic Route to Transition Metal Phosphide Nanoparticles. *Dalton Trans.* **2015**, *44*, 5503–5509. DOI: 10.1039/c4dt03886j.

[31] Yao, Z.; Qiao, X.; Liu, D.; Shi, Y.; Zhao, Y. Catalytic Activities of Transition Metal Phosphides for NO Dissociation and Reduction with CO. *Chem. Biochem. Eng. Q.* **2016**, *29*, 505–510. DOI: 10.15255/CABEQ.2012133.

[32] Guo, L.; Zhao, Y.; Yao, Z. Mechanical Mixtures of Metal Oxides and Phosphorus Pentoxide as Novel Precursors for the Synthesis of Transition-Metal Phosphides. *Dalton Trans.* **2016**, *45*, 1225–1232. DOI: 10.1039/c4dt03886j.

[33] Liang, P.; Liang, F.; Yao, Z.; Gao, H.; Sun, Y.; Jiang, B.; Tong, J. Novel Synthesis of Dispersed Nickel Phosphide Nanospheres on Carbon Support via Carbothermal Reduction Route. *Phosphorus Sulfur Silicon Relat. Elem.* **2017**, *192*, 812–818. DOI: 10.1080/10426507.2017.1286493.

[34] Song, T.; Shi, Y.; Yao, Z.; Gao, H.; Liang, F.; Jiang, B.; Sun, Y.; Kong, L. A Facile Route for Large-Scale Synthesis of Molybdenum Phosphide Nanoparticles with High Surface Area. *Phosphorus Sulfur Silicon Relat. Elem.* **2017**, *192*, 1159–1164. DOI: 10.1080/10426507.2017.1330829.

[35] Liang, L.; Shi, Y.; Yao, Z.; Kang, X.; Jiang, B.; Sun, Y. A Novel Route to the Synthesis of H-ZSM-5-Supported MoP and Ni_2P Phosphides. *Phosphorus Sulfur Silicon Relat. Elem.* **2018**, *193*, 780–786. DOI: 10.1080/10426507.2018.1513519.

[36] Cui, Y.; Liu, Q.; Yao, Z.; Dou, B.; Shi, Y.; Sun, Y. A Comparative Study of Molybdenum Phosphide Catalyst for Partial Oxidation and Dry Reforming of Methane. *Int. J. Hydrogen Energy.* **2019**, *44*, 11441–11447. DOI: 10.1016/j.019.03.170.

[37] Zhao, H.; Shi, Y.; Yao, Z.; Liang, L.; Wang, S.; Liu, Q.; Jiang, B.; Sun, Y. Phenol-Formaldehyde Resin Route to the Synthesis of Several Iron Group Transition Metal Phosphides. *Phosphorus Sulfur Silicon Relat. Elem.* **2019**, *194*, 836–842. DOI: 10.1080/10426507.2018.1550644.

[38] Wang, S.; Cui, Y.; Shi, Y.; Yao, Z.; Liu, Q.; Sun, Y. Alumina-Supported Cobalt Phosphide as a New Catalyst for Preferential CO Oxidation at High Temperatures. *Phosphorus Sulfur Silicon Relat. Elem.* **2019**, *194*, 851–856. DOI: 10.1080/10426507.2019.1571492.

[39] Yao, Z.; Wang, G.; Shi, Y.; Zhao, Y.; Jiang, J.; Zhang, Y.; Wang, H. One-Step Synthesis of Nickel and Cobalt Phosphide Nanomaterials via Decomposition of Hexamethylenetetramine-Containing Precursors. *Dalton Trans.* **2015**, *44*, 14122–14129. DOI: 10.1039/C5DT029J.

[40] Yao, Z.; Wang, L.; Dong, H. A New Approach to the Synthesis of Molybdenum Phosphide via Internal Oxidation and Reduction Route. *J. Alloys Compd.* **2009**, *473*, L10–L12. DOI: 10.1016/j.jallcom.2008.05.048.

[41] Xiao, P.; Sk, M. A.; Thia, L.; Ge, X.; Wang, J.; Lim, K. H.; Lim, R. J.; Wang, X. Molybdenum Phosphide as an Efficient Electrocatalyst for the Hydrogen Evolution Reaction. *Energy Environ. Sci.* **2014**, *7*, 2624–2629. DOI: 10.1039/C4EE00957F.

[42] Burns, A. W.; Gaudette, A. F.; Bussell, M. E. Hydrodesulfurization Properties of Cobalt-Nickel Phosphide Catalysts: Ni-Rich Materials Are Highly Active. *J. Catal.* **2008**, *260*, 262–269. DOI: 10.1016/j.jcat.2008.10.001.

[43] Yao, Z.; Zhang, X.; Peng, F.; Yu, H.; Wang, H.; Yang, J. Novel Highly Efficient Alumina-Supported Cobalt Nitride Catalyst for Preferential CO Oxidation at High Temperatures. *Int. J. Hydrogen Energy.* **2011**, *36*, 1955–1959. DOI: 10.1016/j.ijhydene.2010.11.082.

[44] Qi, Z.; Lee, W. XPS Study of CMP Mechanisms of NiP Coating for Hard Disk Drive Substrates. *Tribol. Int.* **2010**, *43*, 810–814. DOI: 10.1016/j.triboint.2009.11.007.

[45] Perez-Romo, P.; Potvin, C.; Manoli, J.-M.; Chehimi, M. M.; Djéga-Mariadassou, G. Phosphorus-Doped Molybdenum Oxynitredes and Oxygen-Modified Molybdenum Carbides: Synthesis, Characterization, and Determination of Turnover Rates for Propene Hydrogenation. *J. Catal.* **2002**, *208*, 187–196. DOI: 10.1006/jcat.2002.3564.

[46] Guan, Q.; Cheng, X.; Li, R.; Li, W. A Feasible Approach to the Synthesis of Nickel Phosphide for Hydrodesulfurization. *J. Catal.* **2013**, *299*, 1–9. DOI: 10.1016/j.jcat.2012.11.008.

[47] Yao, Z.; Tong, J.; Qiao, X.; Jiang, J.; Zhao, Y.; Liu, D.; Zhang, Y.; Wang, H. Novel Synthesis of Dispersed Molybdenum and Nickel Phosphides from Thermal Carbonization of Metal and Phosphorus-Containing Resins. *Dalton Trans.* **2015**, *44*, 19383–19391. DOI: 10.1039/C5DT02464A.

[48] Chouzier, S.; Afanasiev, P.; Vrinat, M.; Cseri, T.; Roy-Auberger, M. One-Step Synthesis of Dispersed Bimetallic Carbides and Nitrides from Transition Metals Hexamethylenetetramine Complexes. *J. Solid State Chem.* **2006**, *179*, 3314–3323. DOI: 10.1016/j.jssc.2006.06.026.

[49] Ma, D.; Xiao, T.; Xie, S.; Zhou, W.; Gonzalez-Cortes, S. L.; Green, M. L. H. Synthesis and Structure of Bimetallic Nickel Molybdenum Phosphide Solid Solutions. *Chem. Mater.* **2004**, *16*, 2697–2699. DOI: 10.1021/cm035233e.